DALTON
FULL PAPER

Charge transfer salts of tetrathiafulvalene derivatives with magnetic iron(III) oxalate complexes: $[TTF]_7[Fe(ox)_3]_2\cdot 4H_2O$, $[TTF]_5[Fe_2(ox)_5]\cdot 2PhMe\cdot 2H_2O$ and $[TMTTF]_4[Fe_2(ox)_5]\cdot PhCN\cdot 4H_2O$ (TMTTF = tetramethyltetrathiafulvalene)†

Eugenio Coronado, José R. Galán-Mascarós and Carlos J. Gómez-García

*Departamento de Química Inorgánica, Universidad de Valencia, Dr. Moliner 50,
46100 Burjasot, Spain. E-mail: eugenio.coronada@uv.es*

Received 25th August 1999, Accepted 16th November 1999

Three novel TTF (tetrathiafulvalene) and TMTTF (tetramethyltetrathiafulvalene) radical salts of monomeric and dimeric iron(III) oxalate magnetic complexes, $[TTF]_7[Fe(ox)_3]_2\cdot 4H_2O$ **1**, $[TTF]_5[Fe_2(ox)_5]\cdot 2PhMe\cdot 2H_2O$ **2** and $[TMTTF]_4[Fe_2(ox)_5]\cdot PhCN\cdot 4H_2O$ **3**, have been synthesized, and their structures and physical properties investigated. The structures for these semiconducting salts feature monodimensional stackings of the radical cations interleaved by the complexes $[Fe(ox)_3]^{3-}$ and $[Fe_2(ox)_5]^{4-}$, and solvent molecules. For the novel dinuclear complex $[Fe_2(ox)_5]^{4-}$ antiferromagnetic exchange between the two iron atoms through the oxalate bridge was found.

Introduction

One of the most important advantages of molecular-based materials over classic inorganic solids is the possibility to construct new materials that could exhibit in the same crystal lattice combinations of physical properties. Just by using the appropriate molecular building blocks, it may be possible to prepare new solid materials for which electrical, optical and magnetic properties coexist corresponding to two interleaved sub-lattices. Of special interest is the case of coexistence of magnetism and conductivity, or even superconductivity. Superconductivity and magnetism have long been considered inimical to one another,[1] but magnetic superconductors containing 4f elements have been found[2–4] where no significant interactions are present between magnetic and conducting electrons. On the other hand, when interactions between both sub-lattices are present, the possibility to prepare a molecular conducting ferromagnet arises by taking advantage of the ability of the conduction electrons to couple the localized magnetic moments.[5]

In this context, the spatial segregation of anions and cations in the conducting and superconducting charge transfer salts of the organic donor tetrathiafulvalene (TTF) and derivatives is very appealing, since low dimensional packings of the conducting sub-lattice can be obtained with many different anions, including magnetic ones. Using this approach, both types of conducting-magnetic systems described above have been obtained so far. In particular the peculiar magnetic properties of several radical salts of TTF derivatives have been attributed to interactions between π-conduction electrons and localized unpaired d electrons.[6]

The magnetic superconducting salts $[BEDT\text{-}TTF]_4[H_3O][M(ox)_3]\cdot PhCN$ (M = Cr or Fe)[7] and λ-$[BEDT\text{-}TSF]_2[FeCl_4]_{0.5}[GaCl_4]_{0.5}$[6d] have also been reported (BEDT = bis(ethylenedithio)tetrathiafulvalene; BEDT-TSF = bis(ethylene)tetraselenafulvalene). The salts based on oxalate complexes are especially interesting, since the oxalate ion can act as a bridging ligand between transition metals so constructing two-dimensional bimetallic extended structures $[M^{II}M^{III}(ox)_3]_n^{n-}$ which behave as ferro-,[8] ferri-[9] or canted antiferro-magnets.[10] These 2-D anionic layers are usually separated by bulky organic cations XR_4^+ (X = N or P; R = *n*-alkyl or phenyl) or by organometallic cations such as decamethylferrocenium.[11] If we could change this type of cation to TTF derivatives then it might be possible to prepare multilayered materials that could exhibit coexistence of co-operative magnetism and conducting electrons.

With this aim, our first attempts using direct synthetic methods led us to obtain a new family of TTF salts with bimetallic oxalate-bridged trimers of formula $[TTF]_4[M^{II}(H_2O)_2][M^{III}(ox)_3]_2\cdot nH_2O$ (M^{II} = Mn, Fe, Co, Ni, Cu or Zn; M^{III} = Cr or Fe).[12] The use of electrochemical synthesis for this purpose is more desirable, but several problems must be overcome, such as the high insolubility of the inorganic precursors in organic solvents which makes it extremely difficult to find good conditions for crystal growth. With this in mind, the preparation of new salts of TTF derivatives with $[Fe^{III}(ox)_3]^{3-}$ has been explored. This provides the opportunity to determine the structural chemistry resulting from the combination of oxalate complexes with TTFs, offering at the same time the possibility to obtain new compounds combining delocalized electrons and localized magnetic moment.

The present paper reports the synthesis, crystal structures and physical characterization of three new compounds $[TTF]_7[Fe(ox)_3]_2\cdot 4H_2O$ **1**, $[TTF]_5[Fe_2(ox)_5]\cdot 2PhMe\cdot 2H_2O$ **2**, and $[TMTTF]_4[Fe_2(ox)_5]\cdot PhCN\cdot 4H_2O$ (TMTTF = tetramethyltetrathiafulvalene) that behave as semiconductors. The $[Fe(ox)_3]^{3-}$ anion dimerizes in organic solvents to give rise to the novel dinuclear anion $[Fe_2(ox)_5]^{4-}$, one of few examples of Fe^{III}–Fe^{III} oxalate-bridged complexes,[13] and the only one which presents exclusively oxalate ions as ligands.

Results and discussion

Synthesis and structure

As a first step to obtain radical salts of TTF and TMTTF with the magnetic anion $[Fe(ox)_3]^{3-}$ by electrooxidation of the organic donors we needed to solubilize the precursor salt $K_3[Fe(ox)_3].3H_2O$ in organic solvents. Two strategies were tested: (i) the use of a crown ether; and (ii) the extraction of the anion in toluene, using the tetraheptylammonium cation as

---

† Electronic supplementary information (ESI) available: table listing E_i, a_i and b_i values for eqn. (1) and structure labelling schemes. See http://www.rsc.org/suppdata/dt/a9/a906893g/

Table 1 Estimated charges for the TTF and TMTTF molecules present in the radical salts $[TTF]_7[Fe(ox)_3]_2 \cdot 4H_2O$ **1**, $[TTF]_5[Fe_2(ox)_5] \cdot 2PhMe \cdot 2H_2O$ **2** and $[TMTTF]_4[Fe_2(ox)_5] \cdot PhCN \cdot 4H_2O$ **3**

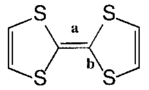

Compound	Molecule type	a/Å	b/Å	$r = a/b$	Q[a]
1	A	1.404(14)	1.71(2)	0.82(2)	1.19(3)
1	B	1.380(9)	1.74(2)	0.793(13)	0.643(10)
1	C	1.393(8)	1.72(2)	0.810(14)	0.99(2)
1	D	1.394(8)	1.72(2)	0.810(14)	0.99(2)
2	A	1.396(11)	1.72(3)	0.81(2)	1.02(3)
2	B	1.35(3)	1.754(7)	0.77(2)	0.173(5)
3	A	1.386(8)	1.72(2)	0.806(14)	0.91(2)
3	B	1.396(7)	1.72(2)	0.812(14)	1.03(2)

[a] $Q = -15.55 + 20.42r$.[15]

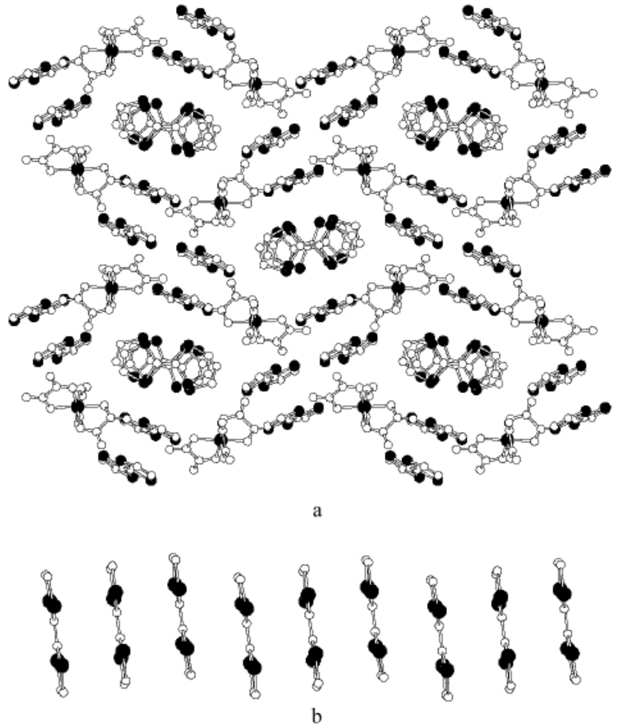
a

b

Fig. 1 (a) View of the structure of the compound $[TTF]_7[Fe(ox)_3]_2 \cdot 4H_2O$ **1** on the *bc* plane. (b) Monodimensional chain of TTF molecules in **1**.

counter ion. This last method, already used in the synthesis of radical salts with other inorganic anionic species, such as polyoxometalates,[14] gave the best results.

Thus, the electrochemical oxidation of TTF in the presence of a toluene solution of $[Fe(ox)_3]^{3-}$ afforded the preparation of two different phases according to the mixture of solvents used in addition to toluene. With dichloromethane, small shiny black crystals of $[TTF]_7[Fe(ox)_3]_2 \cdot 4H_2O$ **1** grew on the electrode. With a benzonitrile–acetonitrile mixture prismatic black crystals of $[TTF]_5[Fe_2(ox)_5] \cdot 2PhMe \cdot 2H_2O$ **2** were obtained. An analogous synthetic process carried out with TMTTF afforded small crystals of $[TMTTF]_4[Fe_2(ox)_5] \cdot PhCN \cdot 4H_2O$ **3**.

The crystal structure of compound **1** shows channels running through the *a* axis formed by the anions and by dimers of TTF molecules. These channels are occupied by chains of TTF molecules (Fig. 1a). The TTF molecules from the dimers are orthogonal to those from the chains. There are four crystallographically independent TTF molecules (A, B, C and D), one of them is located at a centre of symmetry (A) and with molecule B forms the repeating unit for the monodimensional stacking (BAB, Fig. 1b). From the bond distances of each TTF molecule it is possible to estimate the charge:[15] +1 for A, C and D; and +0.5 for B (Table 1), which is in good agreement with the proposed stoichiometry, that implies one A type and two B, C and D type molecules per formula. Thus, molecules C and D are completely charged with strong interactions in the dimer as suggested by short intermolecular S···S contacts (3.26 Å), much shorter than the sum of van der Waals radii (3.6 Å). These cations are interacting also with the $[Fe(ox)_3]^{3-}$ anions, with short S···O contacts (2.90 Å). On the other hand, there is a mixed valence chain with intermolecular distances between 3.41 and 3.48 Å, slightly less than the sum of van der Waals radii, indicating the presence of weak interactions. Of interest is the presence of short contacts between molecule A and the anions (2.94 Å), which suggests electronic localization in the chain. The anions maintain their characteristic octahedral geometry without any significant deviations, and both isomers (Δ and Λ) are present in the crystal. Water molecules fill the holes left by anionic and cationic species, but no hydrogen bonding has been observed.

The structure of compound **2** also contains infinite chains of TTF molecules, which shows the tendency of this kind of molecules to form monodimensional stackings. In this case, the chains running along the *b* axis are surrounded by isolated TTF molecules, solvent molecules (toluene and water) and, surprisingly, by $[Fe_2(ox)_5]^{4-}$ anions (Fig. 2a). These dimers are formed by two octahedral $[Fe(ox)_3]^{3-}$ units sharing an oxalate bridging ligand (Fig. 2b). Analogous dimeric anions have been reported for other metals, such as Cr^{III} and Ni^{II}.[16] The co-ordination geometry of both iron(III) ions deviates from regular octahedral due to the presence of the bridging oxalate. Thus, the Fe–O distances are longer for the shared oxalate (2.09 *vs.* 1.98 Å) and the chelating angle is also shorter (78 *vs.* >84°). These dimers stack forming chains parallel to the TTF ones. Two toluene molecules are located in between the inorganic chains.

There are two independent TTF molecules (A and B): A forms the monodimensional stackings while B is isolated between these chains with its longitudinal axis parallel to the *b* axis. According to the bond distances, the estimate charges would be +1 for A and neutral for B, which is in good agreement with the proposed stoichiometry, since there are four A type and one B type molecules per anion. In the chain (Fig. 2c), A molecules are dimerized with dimers in a zigzag arrangement and very short S···S intradimer distances (3.30 Å). The fact that only A molecules are forming the chains indicates that there will not be electronic delocalization. In addition, intermolecular A···B distances are longer than the sum of van der Waals radii.

The structure of compound **3** consists exclusively of alternating chains of the TMTTF organic donor and the $[Fe_2(ox)_5]^{4-}$ anion running parallel to the [011] direction (Fig. 3a). The cationic chain (Fig. 3b) is formed by two independent TMTTF molecules (A and B), both of them with a charge of +1, as deduced from their respective bond distances, which again is in good agreement with the proposed stoichiometry, since there are two molecules of each type per anion. The organic chain is dimerized with a repeating unit AABB and short intradimer S···S contacts (from 3.30 to 3.38 Å) and longer interdimer contacts (≈3.5 Å). Since all the TMTTF molecules are completely charged and also dimerized, no electronic delocalization is expected for this compound.

On the other hand, the inorganic sublattice is formed by monodimensional stackings of homometallic dimers $[Fe_2(ox)_5]^{4-}$, almost identical to those found in compound **2**, separated in this case by two water and one benzonitrile molecules, with the CN group delocalized between the two positions pointing towards the anions. The dimers are forming hydrogen bonds with surrounding water molecules ($O_{ox} \cdots O_w$ 2.80 Å), but there are no indirect contacts between dimers, which are far enough from each other to assure their magnetic isolation.

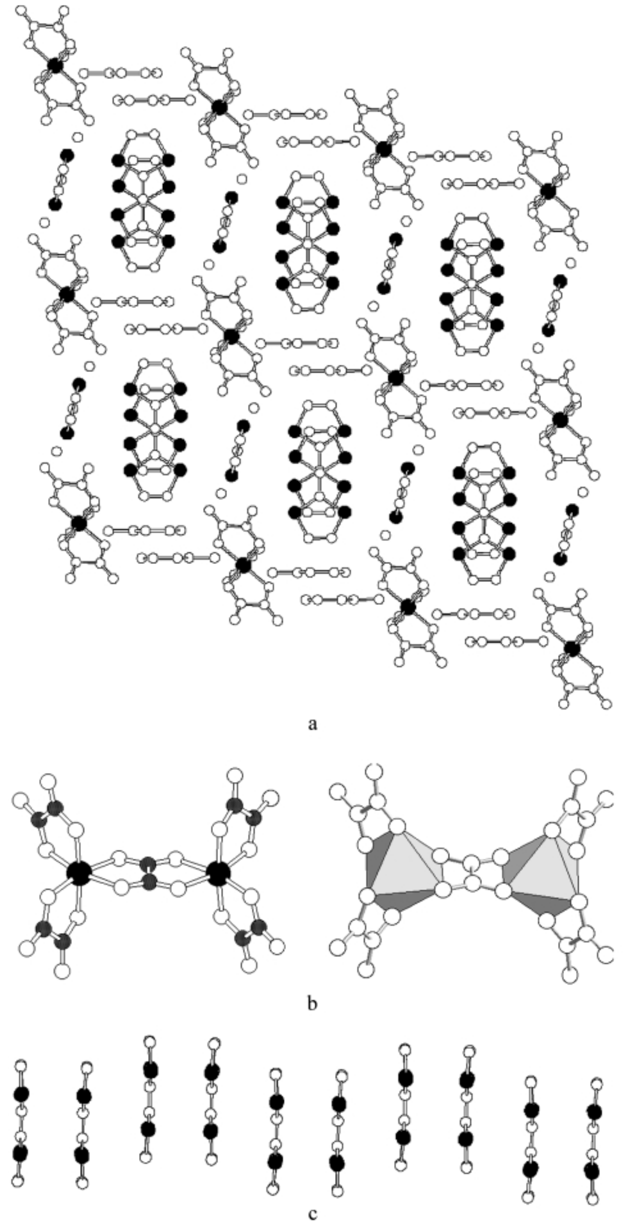

Fig. 2 (a) View of the structure of the compound $[TTF]_5[Fe_2(ox)_5]\cdot 2PhMe\cdot 2H_2O$ **2** on the *ac* plane. (b) View of the dimer $[Fe_2(ox)_5]^{4-}$. (c) Monodimensional chain of TTF molecules in **2**.

Magnetic measurements

Magnetic measurements for compound **1** show a typical paramagnetic behaviour, with the $\chi_m T$ product remaining constant when decreasing the temperature, until at very low temperatures it shows a small decrease. This behaviour obeys a Curie–Weiss law with a Curie constant (C) of 8.45 emu K mol^{-1} that is in good agreement with the expected value for magnetically diluted $[Fe(ox)_3]^{3-}$ complexes (2 units per formula). The small negative Weiss constant ($\theta = -0.44$ K) may be due to a zero field splitting of the iron(III) ions, or to dipolar magnetic interactions between anions. This last possibility should not be significant since the iron(III) ions are more than 9 Å apart from each other. No contribution from the organic sub-lattice is observed, suggesting that the unpaired electrons from the radical cations are strongly coupled, even at room temperature. This was evident for the dimerized TTF molecules as seen in the structural study, and the chain of TTF molecules should be seen as stackings of trimers with no net spin.

Magnetic measurements for compounds **2** and **3** are very similar, and show a maximum in χ_m *vs.* T when the temperature is decreased (Fig. 4), indicating the presence of antiferromagnetic interactions within the dimers. Again, no contribution from the organic sub-lattice is observed in any case, which confirms the conclusions from the structural analysis.

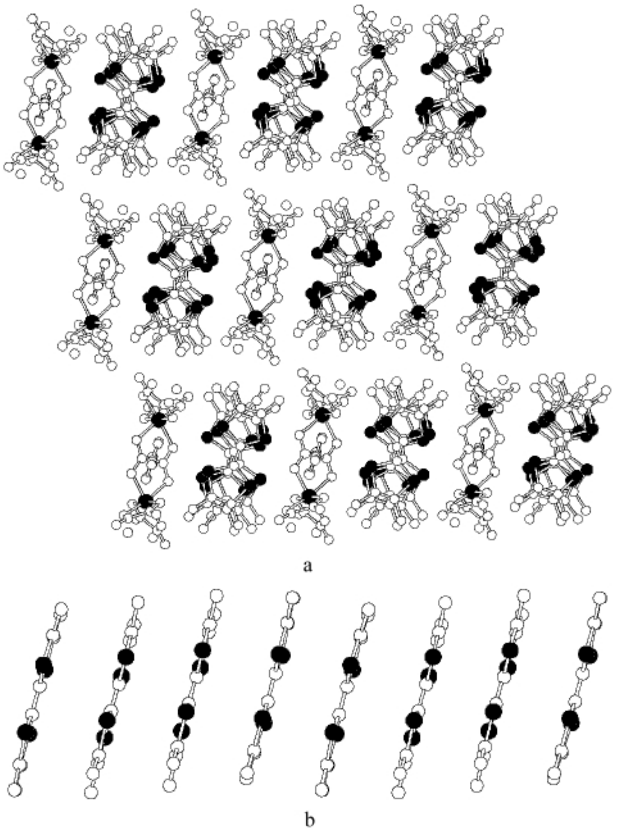

Fig. 3 (a) View of the structure of the compound $[TMTTF]_4[Fe_2(ox)_5]\cdot PhCN\cdot 4H_2O$ **3** showing the stacking of cations and anions in monodimensional chains. (b) Monodimensional chain of TMTTF molecules in **3**.

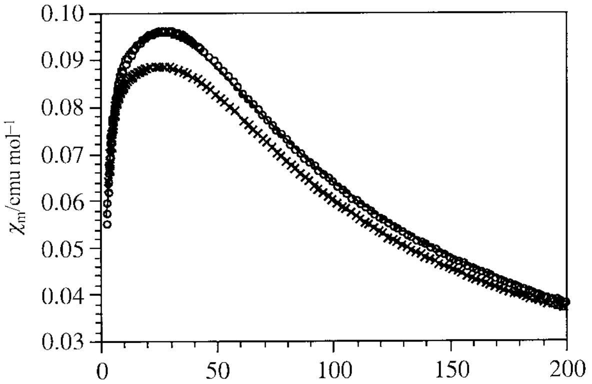

Fig. 4 Magnetic susceptibility as a function of temperature for compounds **2** (empty circles) and **3** (crosses). Solid lines are the best fit by the model (see text).

For these compounds, the magnetic susceptibility as a function of temperature can be fitted by a very simple model of an antiferromagnetically coupled dimer with an exchange interaction J between iron(III) ions. The exchange Hamiltonian can be expressed as $H_{ex} = -2JS_1S_2$, where $S_1 = S_2 = 5/2$. For this kind of system,[17] the energy levels can be expressed as a function of J: $E_i = -J[S_T(S_T + 1) - S_1(S_1 + 1) - S_2(S_2 + 1)]$, where $S_T = |S_1 + S_2| \ldots |S_1 - S_2| = 5, 4, 3, 2, 1$ or 0. Finally, the susceptibility is obtained with the Van Vleck equation to which a new term is added corresponding to a possible paramagnetic impurity (C'/T), commonly found in radical salts due to defects from the organic sub-lattice,[18] eqn. (1) (E_i, a_i and b_i values can be found

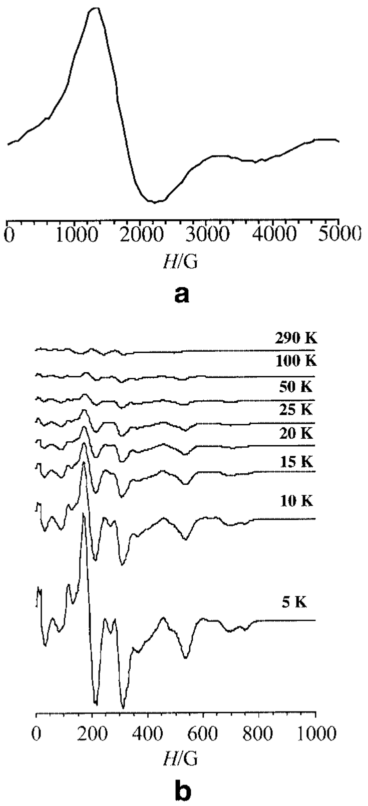

Fig. 5 (a) Room temperature EPR spectrum for the salt $K_3[Fe(ox)_3]\cdot 3H_2O$. (b) Variable temperature EPR spectra for the salt $[TTF]_7[Fe(ox)_3]_2\cdot 4H_2O$ **1**.

$$\chi_m = \left(\frac{Ng^2\mu^2}{k_BT}\right)\frac{\Sigma_i a_i \exp(-E_i/k_BT)}{\Sigma_i b_i \exp(-E_i/k_BT)} + \frac{C'}{T} \qquad (1)$$

in the ESI). With this model the maximum in χ_m around 35 K for **2** and **3** is perfectly reproduced with values of J (−3.57 and −3.69 cm^{-1}, respectively) and g (2.01 and 1.96) very similar in the two cases, and a small paramagnetic impurity contribution (≈0.1 emu K mol^{-1}). These J values are in good agreement with those observed for the other two known examples of Fe^{III}–Fe^{III} oxalate-bridged complexes (−3.61 cm^{-1} for $[Fe_2(acac)_2(ox)]\cdot\frac{1}{2}H_2O$ and −3.84 cm^{-1} for $[NEt_4]_4[Fe_2(NCS)_8(ox)]$).[13]

EPR spectroscopy

The EPR spectrum of the precursor salt $K_3[Fe(ox)_3]\cdot 3H_2O$ (Fig. 5a) shows a very anisotropic signal with two different bands centred at $g = 3.8$ and 1.8. The intensity of the signal increases when the temperature is lowered, although no fine structure for the spectra is observed due to the dipolar broadening because of the proximity between magnetic centres.

The spectrum for compound **1** (Fig. 5b), containing the same monomer $[Fe(ox)_3]^{3-}$, shows also a signal centred at a similar field ($g = 3.5$), which increases its intensity when the temperature is lowered. However, in this case the fine structure is observed since in this compound the anion is magnetically diluted. The complexity of this signal arises from the weak anisotropy of the spin $S = 5/2$, which gives rise to a zero field splitting, with a D parameter $\ll h\nu = 0.3$ cm^{-1}. According to the literature,[19] this spectrum would correspond to a D value about 0.2 cm^{-1}. As stated in the published studies, the signal for this anion depends dramatically on the nature of the counter ions, since small variations in the local geometry of the coordination sphere results in big differences between the EPR spectra.

The most interesting observation from the spectra of compound **1** is the absence of an EPR signal from the organic sub-lattice in the temperature range studied. This confirms that the electrons are strongly coupled in each TTF dimer, and also in the chain, as suggested by the magnetic measurements.

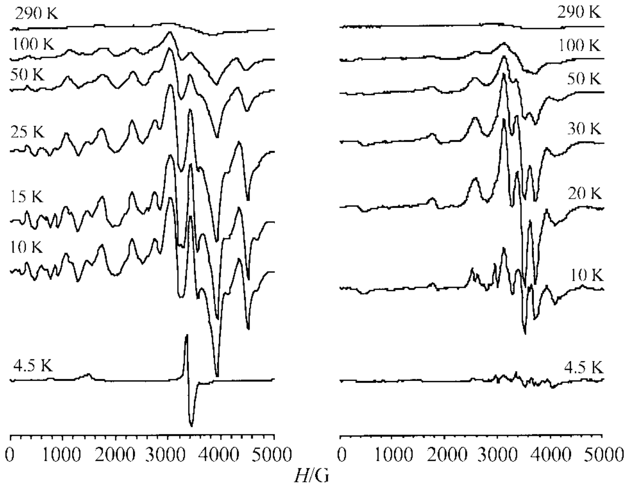

Fig. 6 Variable temperature EPR spectra for the salts $[TTF]_5[Fe_2(ox)_5]\cdot 2PhMe\cdot 2H_2O$ **2** (left) and $[TMTTF]_4[Fe_2(ox)_5]\cdot PhCN\cdot 4H_2O$ **3** (right).

As expected, the EPR spectra for compounds **2** and **3** are completely different to those of **1**, showing several signals corresponding to the $[Fe_2(ox)_5]^{4-}$ dimer (Fig. 6). The spectra are very similar in the two cases. The higher intensity for **2** allows us to observe small bands at low fields that cannot be observed for **3**. According to the magnetic measurements, the ground state for this dimer is $S = 0$, and the excited states ($S = 1, 2, \ldots$) are far enough from this ground state to avoid the observation of transitions between different energy levels (the estimated energy difference between $S = 0$ and the first excited state $S = 1$ should be larger than 7 cm^{-1}). The main signal centred at $g = 1.9$ should correspond to a transition within the first excited $S = 1$ state, since its intensity increases when the temperature is lowered, reaches a maximum intensity and then decreases, disappearing at very low temperatures when only the ground state is populated. In addition, the shape for this signal, better observed for **3**, is that expected for a spin triplet (6 bands). The weaker signals that appear at lower fields show also a decrease at very low temperatures and disappear at higher temperatures than the main signal. Thus, these signals should correspond to transitions within excited states of higher energy ($S = 2, 3, \ldots$). Although some of these last signals are slightly similar to that of the monomer, they cannot be derived from impurities in these compounds, since a typical paramagnetic signal from the monomer, as seen before for **1**, would increase its intensity monotonically without reaching any maximum.

No signal coming from the organic sub-lattice is expected for compound **3**, but there is indeed a symmetric and narrow signal centred at $g = 2.01$ corresponding to TTF cations. This signal shows a paramagnetic behaviour, since its intensity increases when the temperature is lowered, being the predominant signal at very low temperatures where those coming from the dimer disappear. It should be stressed that this paramagnetic impurity observed in the organic sub-lattice is very small and has to be related to the paramagnetic contribution C', introduced in the fit of the magnetic susceptibility measurements.

Electrical conductivity

The conductivity measurements on single crystals for these radical salts are similar in all cases. The room temperature conductivity for **1** is 10^{-4} S cm^{-1}, and it behaves as a semiconductor with quite high activation energy, 279 meV. This confirms that the electrons from the organic sub-lattice are strongly localized. The room temperature conductivity for **2** is 1.8×10^{-6} S cm^{-1}, typical of an insulator. This result is also in good agreement

Table 2 Crystallographic data and structural refinement for $[TTF]_7[Fe(ox)_3]_2\cdot 4H_2O$ **1**, $[TTF]_5[Fe_2(ox)_5]\cdot 2PhMe\cdot 2H_2O$ **2** and $[TMTTF]_4[Fe_2(ox)_5]\cdot PhCN\cdot 4H_2O$ **3**

Formula	$C_{54}H_{36}Fe_2O_{28}S_{28}$	$C_{54}H_{40}Fe_2O_{22}S_{20}$	$C_{57}H_{56}Fe_2NO_{24}S_{16}$
Formula weight	2142.2	1793.73	1763.68
T/K	293(2)	293(2)	293(2)
Space group	$P2_1/c$	$C2/m$	$P\bar{1}$
a/Å	10.487(2)	19.777(9)	11.610(2)
b/Å	21.118(11)	13.900(2)	14.085(2)
c/Å	17.514(2)	13.457(2)	14.253(2)
α/°			118.110(2)
β/°	94.56(2)	107.40(2)	90.660(2)
γ/°			114.100(2)
V/Å^3	3866(2)	3530(2)	1815.4(2)
Z	2	2	1
μ(Mo-Kα)/cm^{-1}	12.12	10.77	9.35
Reflections/independent	7560/6974	3380/3221	7268
$I > n\sigma(I)$	4	6	4
Reflections/parameters	3647/506	1485/231	4709/399
R_{int}	0.0280	0.0484	0.0298
$R1^a$	0.0459	0.0501	0.0490
$R2$	0.0976	0.1347	0.1154

with the structural and magnetic measurements, since it contains a chain of TTF dimers, with the electrons localized in each dimer, and isolated neutral TTF molecules. Finally, the room temperature conductivity found for **3** is the highest one, 2.2×10^{-3} S cm^{-1}, and it also behaves as a semiconductor with a high activation energy, 290 meV.

Conclusion

We have presented three novel radical salts based upon TTF and its derivative TMTTF using as counter ion magnetic oxalate complexes of Fe^{III}. All of them show one-dimensional stackings of the organic radicals placed in the channels formed by the complex anions, isolated organic donors and solvent molecules.

From the chemical point of view, it is interesting that the complex $[Fe(ox)_3]^{3-}$ dimerizes in organic solvents (benzonitrile–acetonitrile mixtures) to yield the anion $[Fe_2(ox)_5]^{4-}$, which shows strong antiferromagnetic pairwise interactions between both metal centres, as demonstrated by magnetic measurements and EPR spectroscopy.

The high electronic localization in the organic sub-lattices, as supported by the structural features is responsible for the semiconducting behaviour observed in these hybrid radical salts which show low conductivities and high activation energies.

Experimental

Materials

The precursor salt $K_3[Fe(ox)_3]\cdot 3H_2O$ was prepared according to the literature method,[20] TTF was used as purchased, and TMTTF was supplied by Professor Pierre Delhaes from the Centre de Recherche Paul Pascal of Bordeaux (France).

Preparations

Extraction of the $[Fe(ox)_3]^{3-}$ anion in toluene. In a sintered funnel an aqueous solution (100 mL) of $K_3[Fe(ox)_3]\cdot 3H_2O$ (4.87 g, 10 mmol) and a toluene solution (100 mL) of $[N(C_7H_{15})_4]Br$ (9.80 g, 20 mmol) were mixed. After several minutes of continuous stirring the anion was transferred to the organic phase, which acquires a characteristic yellow colour, and the underlying aqueous solution was discarded. In order to assure that no Br$^-$ remains in the organic solution (that could favour the formation of bromide salts of the organic radical cations), this process was repeated by adding to the funnel a new aqueous solution of $K_3[Fe(ox)_3]\cdot 3H_2O$ (4.87 g, 10 mmol). After this second extraction the toluene solution was directly used in the electrochemical syntheses.

$[TTF]_7[Fe(ox)_3]_2\cdot 4H_2O$ 1. In the anodic compartment of a U-shape electrocrystallization cell TTF (0.01 g, 0.05 mmol) was dissolved in dichloromethane (10 mL) and then the iron anion extracted in toluene (2 mL) was added. To a similar mixture of solvents in the cathodic compartment several drops of water were added, and by electrooxidation of the TTF at a low and constant current ($I = 0.5$ µA) small shiny black crystals were grown on a platinum wire. After two weeks the crystals were filtered off, washed thoroughly with dichloromethane and dried in the dark.

$[TTF]_5[Fe_2(ox)_5]\cdot 2C_6H_5Me\cdot 2H_2O$ 2. With the same procedure, but using as solvent benzonitrile–acetonitrile (6:4 mL) instead of dichloromethane in the preparation of the solutions and with the same current, small black crystals were grown on the platinum wire. After three weeks the crystals were filtered off, washed with acetonitrile and dried in the dark.

$[TMTTF]_4[Fe_2(ox)_5]\cdot PhCN\cdot 4H_2O$ 3. In the anodic compartment of a U-shape electrocrystallization cell TMTTF (0.01 g, 0.04 mmol) was dissolved in benzonitrile–acetonitrile (6:4 mL) and then the iron anion extracted in toluene (2 mL) was added. To a similar mixture of solvents in the cathodic compartment several drops of water were added, and by electrooxidation of the TMTTF at a low and constant current ($I = 0.5$ µA) prismatic shiny black crystals were grown on the platinum wire. After two weeks the crystals were filtered off, washed with acetonitrile and dried in the dark.

Structural determination

From the platinum wires on which they had grown, a small shiny square prismatic black crystal of **1**, a shiny black needle of **2**, and a rhombohedral plate of **3** were collected and used for X-ray analysis. The three structures were solved by direct methods using the SIR 97 program,[21] and refined on F^2 using the SHELXL 97 program.[22] The positions of the hydrogen atoms were calculated in all cases. All atoms were refined anisotropically except hydrogens.

Crystallographic data and refinement parameters are summarized in Table 2.

CCDC reference number 186/1738.

See: http://www.rsc.org/suppdata/dt/a9/a906893g/ for crystallographic files in .cif format.

Magnetic measurements

Magnetic susceptibility measurements were carried out on polycrystalline samples between 2 and 300 K in the presence of a magnetic field between 0.1 and 1 T in a magnetometer

(Quantum Design MPMS-XL-5) equipped with a SQUID sensor. Diamagnetic contributions were deduced and corrected using diamagnetic Pascal constants.

ESR spectroscopy

Measurements were performed between 4.2 and 300 K with a X-band spectrometer (Bruker 200D) equipped with a liquid helium cryostat.

Electrical conductivity

Electrical conductivities were measured on single crystals with a Keithley 224 current source capable of generating a continuous current between 5 μA and 0.1 A, and with a Keithley 199 microvoltmeter, with a maximum sensibility of 1 μV. As cryostat, the equipment from the SQUID magnetometer (Quantum Design MPMS-XL-5) was used.

Acknowledgements

We thank The Ministerio de Educación y Cultura (MEC) and The Generalitat Valenciana (GV) for the financial support to purchase a SQUID magnetometer. This work was supported by the MEC (Grant PB96-0862). J. R. G.-M. thanks the GV for a predoctoral fellowship.

References

1 See *Topics in Current Physics*, eds. Ø. Fisher and M. B. Maple, Springer, New York, 1983, vols. 32, 34.

2 M. Ishikawa and Ø. Fisher, *Solid State Commun.*, 1977, **23**, 37; J. W. Lynn, G. Shirane, W. Thomlinson and R. N. Sheldon, *Phys. Rev. Lett.*, 1981, **46**, 368.

3 W. A. Fertig, D. C. Johnson, L. E. DeLong, R. W. McCallum, M. B. Maple and B. T. Matthias, *Phys. Rev. Lett.*, 1977, **38**, 987; D. E. Moncton, D. B. McWhann, P. H. Schmidt, G. Shirane, W. Thomlinson, M. B. Maple, H. B. MacKay, L. D. Woolf, Z. Fisk and D. C. Johnson, *Phys. Rev. Lett.*, 1980, **45**, 2060.

4 K. M. Beauchemp, G. C. Spalding, W. H. Huber and A. M. Goldman, *Phys. Rev. Lett.*, 1994, **73**, 2752.

5 E. Coronado, R. Georges and B. S. Tsukerblat, in *Molecular Magnetism: From Molecular Assemblies to the Devices*, eds. E. Coronado, P. Delhaes, D. Gatteschi and J. S. Miller, NATO ASI Series, Kluwer Academic Press, Dordrecht, 1996, vol. 321, p. 105.

6 (*a*) P. Batail, L. Ouahab, J. B. Torrance, M. L. Pylman and S. S. P. Parkin, *Solid State Commun.*, 1985, **55**, 597; (*b*) R. Kumai, A. Asamitsu and Y. Tokura, *Chem. Lett.*, 1996, 753; (*c*) M. Y. Ogawa, J. Martinsen, S. M. Palmer, J. L. Stanton, J. Tanaka, R. Greene, B. M. Hoffman and J. A. Ibers, *J. Am. Chem. Soc.*, 1987, **109**, 1115; (*d*) H. Kobayashi, H. Tomita, T. Naito, A. Kobayashi, F. Sakai, T. Watanabe and P. Cassoux, *J. Am. Chem. Soc.*, 1996, **118**, 368; (*e*) E. Coronado, L. R. Falvello, J. R. Galán-Mascarós, C. Giménez-Saiz, C. J. Gómez-García, V. N. Lauhkin, A. Pérez-Benítez, C. Rovira and J. Veciana, *Adv. Mater.*, 1997, **9**, 984.

7 A. W. Graham, M. Kurmoo and P. Day, *J. Chem. Soc., Chem. Commun.*, 1995, 2061; M. Kurmoo, A. W. Graham, P. Day, S. J. Coles, M. B. Hursthouse, J. L. Caulfield, J. Singleton, F. L. Pratt, W. Hayes, L. Ducasse and P. Guioneau, *J. Am. Chem. Soc.*, 1995, **117**, 12209; L. Martin, S. S. Turner, P. Day, K. M. Abdul-Malik, S. J. Coles and M. B. Hursthouse, *Chem. Commun.*, 1999, 513.

8 H. Tamaki, Z. J. Zhong, N. Matsumoto, S. Kida, M. Koikawa, N. Achiwa, Y. Hashimoto and H. Okawa, *J. Am. Chem. Soc.*, 1992, **114**, 6974.

9 H. Tamaki, M. Mitsumi, K. Nakamura, N. Matsumoto, S. Kida, H. Okawa and S. Iijima, *Chem. Lett.*, 1992, 1975; H. Okawa, N. Matsumoto, H. Tamaki and M. Ohba, *Mol. Cryst. Liq. Cryst.*, 1993, **233**, 257; J. Larionova, B. Mombelli, J. Sanchez and O. Kahn, *Inorg. Chem.*, 1998, **37**, 679.

10 C. Mathonière, S. G. Carling, D. Yusheng and P. Day, *J. Chem. Soc., Chem. Commun.*, 1994, 1551; C. Mathonière, J. Nuttall, S. G. Carling and P. Day, *Inorg. Chem.*, 1996, **35**, 1201.

11 M. Clemente-León, E. Coronado, J. R. Galán-Mascarós and C. J. Gómez-García, *Chem. Commun.*, 1997, 1727.

12 E. Coronado, J. R. Galán-Mascarós, C. Giménez-Saiz, C. J. Gómez-García, C. Ruiz-Pérez and S. Triki, *Adv. Mater.*, 1996, **8**, 737.

13 M. Julve and O. Kahn, *Inorg. Chim. Acta*, 1983, **76**, L39; S. Triki, F. Bérézovsky, J. S. Pala, E. Coronado, C. J. Gómez-García, A. Riou and P. Molinié, *Inorg. Chem.*, in the press.

14 M. Clemente-Léon, E. Coronado, J. R. Galán-Mascarós, C. Giménez-Saiz, C. J. Gómez-García and T. Fernández-Otero, *J. Mater. Chem.*, 1998, **8**, 309.

15 T. C. Umland, S. Allie, T. Kuhlmann and P. Coppens, *J. Phys. Chem.*, 1988, **92**, 6456.

16 V. M. Masters, C. A. Sharrad, P. V. Bernhardt, L. R. Gahan, B. Moubaraki and K. S. Murray, *J. Chem. Soc., Dalton Trans.*, 1998, 413; P. Román, C. Guzmán-Miralles, A. Luque, J. I. Beitia, J. Cano, F. Lloret, M. Julve and S. Alvarez, *Inorg. Chem.*, 1996, **35**, 3741.

17 E. W. Hatfield, *Theory and Applications of Molecular Paramagnetism*, Wiley, New York, 1976.

18 C. Bellito, M. Bonamico, V. Fares, F. Federici, G. Righini, M. Kurmoo and P. Day, *Chem. Mater.*, 1995, **7**, 1475; C. J. Gómez-García, C. Giménez-Saiz, S. Triki, E. Coronado, P. Le Magueres, L. Ouahab, L. Ducasse, C. Sourisseau and P. Delhaes, *Inorg. Chem.*, 1995, **34**, 4139.

19 D. Collison and A. K. Powell, *Inorg. Chem.*, 1990, **29**, 4735.

20 J.-C. Baylar and E. M. Jones, in *Inorganic Synthesis*, ed. H. S. Booth, McGraw-Hill, New York, 1939, vol. 1, p. 35.

21 SIR97, A. Altomare, M. C. Burla, M. Camalli, G. Cascarano, C. Giacovazzo, A. Guagliardi, A. G. G. Moliterni, G. Polidori and R. Spagna, *J. Appl. Crystallogr.*, 1999, **32**, 115.

22 SHELXL 97, G. M. Sheldrick, University of Göttingen, 1997.

Paper a906893g